

Vortex Wake and Energy Transitions of an Oscillating Cylinder at Low Reynolds Number

B.E. Stewart, J.S. Leontini, K. Hourigan and M.C. Thompson

Department of Mechanical Engineering
Monash University, Victoria, 3800 AUSTRALIA

Abstract

As a means of understanding the phenomenon of vortex-induced vibration, the forced oscillation of a cylinder in cross-flow has been examined. A lack of information regarding the connections between energy transfer and the wake mode of oscillating bodies in low Reynolds number flow prompted a two-dimensional numerical investigation at $Re = 200$. The region in which vortex shedding synchronized with the cylinder forcing frequency was defined and the energy transfer calculated. The mode of Kármán vortex shedding incorporated a gradual change from positive to negative energy transfer as the amplitude of the motion was increased. A mode of shedding was detected in the negative energy region in which a pair and a single vortex (P+S) were shed each motion cycle. Energy contours were established in the region of primary lock-in and the boundary of zero energy transfer was defined.

Introduction

The phenomenon of vortex-induced vibration (VIV) has been studied in some detail over recent years with a common approach being to investigate the near wake and energy transfer characteristics of a bluff body undergoing forced cross-flow oscillation (see reviews in [11]). This approach provides a valuable indication of flow regimes likely to result in VIV. Modern advances in robotics and nano-technology are yielding fluid immersed structures with small characteristic length scales, resulting in low Reynolds number flow regimes. This underlines the need for a greater understanding of the energy transfer characteristics of flows at $Re < 350$.

The current numerical investigation attempts to define the region of positive energy transfer for a cylinder undergoing forced oscillation transverse to the flow at a Reynolds number of 200. Experimentation has found that forcing a cylinder to oscillate transverse to a flow caused the vortex shedding of the cylinder to synchronize with the imposed motion along its entire length [7]. In this way, oscillations near the natural shedding frequency, f_n , extended the laminar flow range from $Re = 150$ to approximately 350 [7,4], resulting in physical flows that could be accurately approximated by two-dimensional simulations. This region of synchronisation or 'lock-in' near f_n is termed the primary (or fundamental) lock-in region and the boundaries are dependent on Re [5]. For frequencies away from f_n , the flow becomes chaotic and at certain values of amplitude and frequency, synchronisation may be difficult to determine [9].

An examination of the wake at various amplitudes of oscillation was conducted in order to determine specific regions of the near wake influencing the direction of energy transfer. As vortices are shed from the structure, vortex formation takes place from the interaction of four regions of vorticity generated at the body during each motion cycle [12,2]. These regions may then interact to shed two, three or four vortices into the wake each cycle. For oscillations near the fundamental lock-in region, a wake mode shedding two pairs of opposite sign vortices (2P) has been observed [12], but for flows with Re less than 300 this mode is replaced by a pair and a single vortex (P+S) being shed [2,7,5].

More complex modes have been detected at harmonics and sub-harmonics of f_n with the wake being encouraged to lock-on at these frequencies [1,12]. During their investigation, Griffin and Ramberg [5] concluded that the appearance of the P+S wake at higher amplitudes was linked to a transition from a drag induced wake to a jet (where thrust dominated). At $Re \leq 200$ this wake mode was predicted and observed within the synchronization region at amplitudes of oscillation greater than 0.65 cylinder diameters [5,9].

Carberry et al. [3] found experimentally that changes in the lift force, and hence the energy transfer, of a cylinder undergoing forced oscillation was intrinsically linked to the formation of the near wake. When traversing the parameter space defined by frequency versus amplitude of the body motion, a discontinuity in the phase between the lift force and cylinder displacement was perceived. This discontinuity was commented upon by Bishop and Hassan [1] and has since been observed at frequencies both above and below the natural shedding frequency at a range of Reynolds numbers [8,6,2]. Difficulties in detecting the phase jump at low Reynolds number led Blackburn and Henderson [2] to conclude that flows at $Re < 400$ have viscous dissipation inhibiting the switch and only for values of Re greater than this can the phenomenon be accurately observed. The phase jump is often associated with a change in sign of energy transfer or shedding mode and when the phase between cylinder displacement and lift force was observed to jump through 180° the direction of energy transfer changed from positive to negative [9,3,12,2,1]. Hover et al. [6] have reproduced energy transfer contours from data at $Re = 3800$ and 10000 in the non-dimensional amplitude-frequency plane. The authors found that the contour of zero energy transfer agreed reasonably with the data obtained from free vibration of the cylinder at $Re = 3800$. This result indicated that analysis of forced vibration might be a useful tool for predicting the regions in which vortex induced vibration is possible and provide an upper limit for the amplitude of oscillation.

Computational Methodology

The cylinder motion was described by the relationship

$$y(t) = A \cos(2\pi f_o t), \quad (1)$$

where A is the amplitude of displacement and f_o is the forcing frequency. Results are described in terms of the scaled amplitude, A/D and the reduced velocity

$$V_r = \frac{U}{f_o D}, \quad (2)$$

which is equivalent to the wavelength of the cylinder motion scaled by D . Attention was focused on the primary lock-in region of the parameter space. Throughout the investigation, the scaled amplitude was varied between 0.1 and 1.0 and the reduced velocity between 1.0 and 8.0. No fewer than 80 data sets were collected at irregularly spaced intervals throughout this region. The cylinder was constrained to move transverse to the up stream flow and hence the drag force played no part in the energy transfer. Analysis of the drag force was therefore neglected throughout this study.

Also used to characterise the wake was the Strouhal frequency

$$St = \frac{f_n D}{U}. \quad (3)$$

Data analysis was carried out using the lift coefficient, C_L , and non-dimensional energy transfer per motion cycle,

$$E = -\frac{1}{D} \int_0^T A \sin(2\pi f_o t) C_L(t) dt, \quad (4)$$

as defined in [2]. E indicates the component of C_L in phase with the cylinder velocity over one period of motion T and positive E indicates work done by the fluid on the cylinder. The energy integral given by equation (4) was evaluated using a composite Simpson's Rule. For consistency, the time was scaled by U/D , giving dimensionless time τ .

Numerical Code

The two-dimensional numerical code utilized a spectral-element scheme with three-step time splitting to solve the incompressible Navier-Stokes equations with an additional forcing term. Eighth-order Lagrangian interpolating polynomials were used to approximate the solution variables within the macro-elements of the mesh. For a more detailed description of the numerical scheme see [10]. The mesh (shown in figure 1) consisted of quadrilateral elements with the domain extending $23D$ downstream and $15D$ upstream and to each of the transverse boundaries. The mesh was attached to the non-inertial frame of reference of the cylinder and the free-stream flow and cylinder motion were started impulsively from rest. A no-slip condition was enforced at the cylinder body.

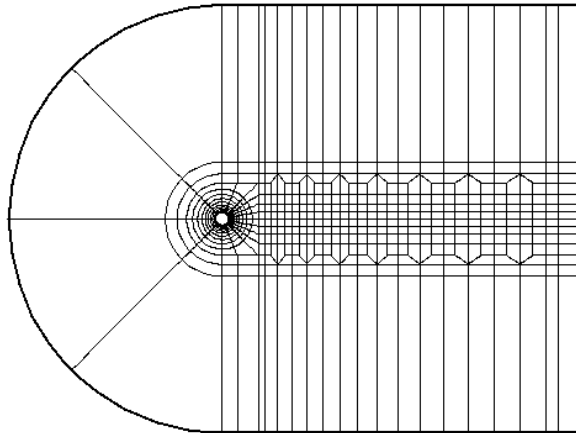


Figure 1. Macro-element mesh used during investigation

Detailed resolution and convergence tests have previously been conducted for this system at a variety of Reynolds numbers and were found to give results that compared well with accepted values [10]. For completeness, a time-step analysis was carried out for the fixed and forced cylinders in the current investigation. Time-steps of $\Delta\tau = 0.001$ and 0.002 were used to check convergence of the solution. In the case of the fixed cylinder, the smaller time-step led to a slightly faster flow development but the vortex shedding frequency for the two solutions was found to be identical to 5 significant figures over any defined time interval. In the case of the cylinder undergoing forced oscillations, the flow development was dictated by the cylinder motion and the lift and drag coefficients were within 0.1% after $\tau = 200$. Consequently $\Delta\tau = 0.001$ was deemed to give sufficient accuracy and was used

in all subsequent simulations. A fixed cylinder simulation run at $Re = 200$ for $\tau > 350$ provided the natural shedding frequency of the cylinder. Using an FFT over the entire lift force data series, equation (3) gave $St = 0.198$.

Results

The wake was considered synchronized with the cylinder motion when a plot of cylinder displacement versus lift traced out a steady, closed loop (see [2]) and the energy transfer per cycle had reached a constant value. For certain forcing frequencies near f_n , synchronization was difficult to obtain, with a small variation in the frequency altering the lift data from a steady synchronized form to a slowly varying series with a small constant increase in E each cycle. This behaviour continued for $\tau > 500$ with no sign of stabilising. Such sensitivity of cylinder wakes near the Strouhal frequency has been observed in previous numerical investigations [2,9].

At reduced velocities below 4.5, wake visualisations showed an apparently stable Kármán wake; however a prominent beating was present between f_o and f_n . Although the forcing frequency was dominant, the interaction of these two frequencies led to a beating in the form of the energy transfer per motion cycle and E consequently varied about a mean value. The varying nature of the energy transfer led this region to be classified as non-synchronised. Areas in which this chaotic nature was particularly apparent were at $3f_n$ and $3/2f_n$ and near these frequencies the energy transfer oscillated about a mean value that was becoming increasingly negative. Again, very long time-scale simulations were necessary to determine an equilibrium state. As V_r increased to values near 4.5, the vortex shedding locked on. This occurred first at amplitudes above 0.5 where the effects of cylinder motion were more pronounced. As f_o approached f_n synchronisation occurred at all values of A/D . This lock-on was observed throughout the parameter space until $V_r > 6.5$, at which point the wake pattern become totally chaotic. This boundary coincided closely with that established by Williamson and Roshko [12], defining the limits of the fundamental synchronization region.

As the amplitude of oscillation was increased from a value of 0.2 in the synchronization region, the lift trace varied continuously from a sinusoidal trace, out of phase with the cylinder displacement, to an asymmetric mode becoming apparent at values of $A/D > 0.6$. This represented the progression from the standard Kármán street wake to the P+S mode of shedding. Kármán shedding occurred at low amplitudes and displayed a gradual change from positive to negative energy transfer with increasing amplitude. P+S shedding was observed only in the region of negative energy transfer.

Lift data is shown along with cylinder displacement for $V_r = 5.0$ at three different amplitudes within the lock-on region (figure 2). It was apparent that although the lift phase experienced a shift between the Kármán shedding in figure 2(d) and the P+S shedding in figure 2(f), the wake mechanism governing this shift was not obvious. During the Kármán shedding the lift progressed from a near sinusoidal trace to one that contained two smaller, secondary peaks per oscillation (figure 2(b)). These peaks became apparent at amplitudes between 0.40 and 0.45 in the primary lock-on region. The flow remained symmetric with secondary maxima and minima developing in the lift trace each cycle. Following the development of the secondary peaks an increase in the amplitude caused the major peaks and troughs to reduce until all were of approximately equal magnitude. Further increases in A/D caused a growth in alternate peaks, creating a phase shift between lift and displacement. At this time the wake was still symmetric and shedding in the Kármán street mode. An

increase in amplitude following this switch led to the disappearance of one of the remaining secondary peaks (figure 2(c)) and the development of the asymmetric, P+S mode mentioned previously. One such peak transition occurred at the time indicated by dots in figure 2(a), (b) and (c) at which wake images were obtained. The phase shift corresponded to a change in the direction of energy transfer. Although the switch occurred as the result of a continuous process, the transition took place over a small amplitude range and was completed within a variation of $A/D < 0.1$. At the time that images were obtained the cylinder was at maximum downward velocity and the lift data changed dramatically from an extreme negative in figure 2(a) to almost zero in (b) and an extreme positive in (c).

Three dominant pressure regions affected the lift force on the cylinder. These were the high pressure area at the front stagnation point and the low pressure regions corresponding to the top and bottom shear layers, occurring just before separation. As the amplitude was increased these points were displaced further around the cylinder during maximum velocity (as shown by the high and low pressure regions indicated in figure 2(d), (e) and (f)). This shift made a substantial difference in the overall lift when the pressure forces at the top and bottom of the cylinder were nearly balanced.

In figure 2(d) the cylinder's downward motion caused acceleration of the lower shear layer which created an area of low pressure near the bottom of the cylinder and a net downward lift

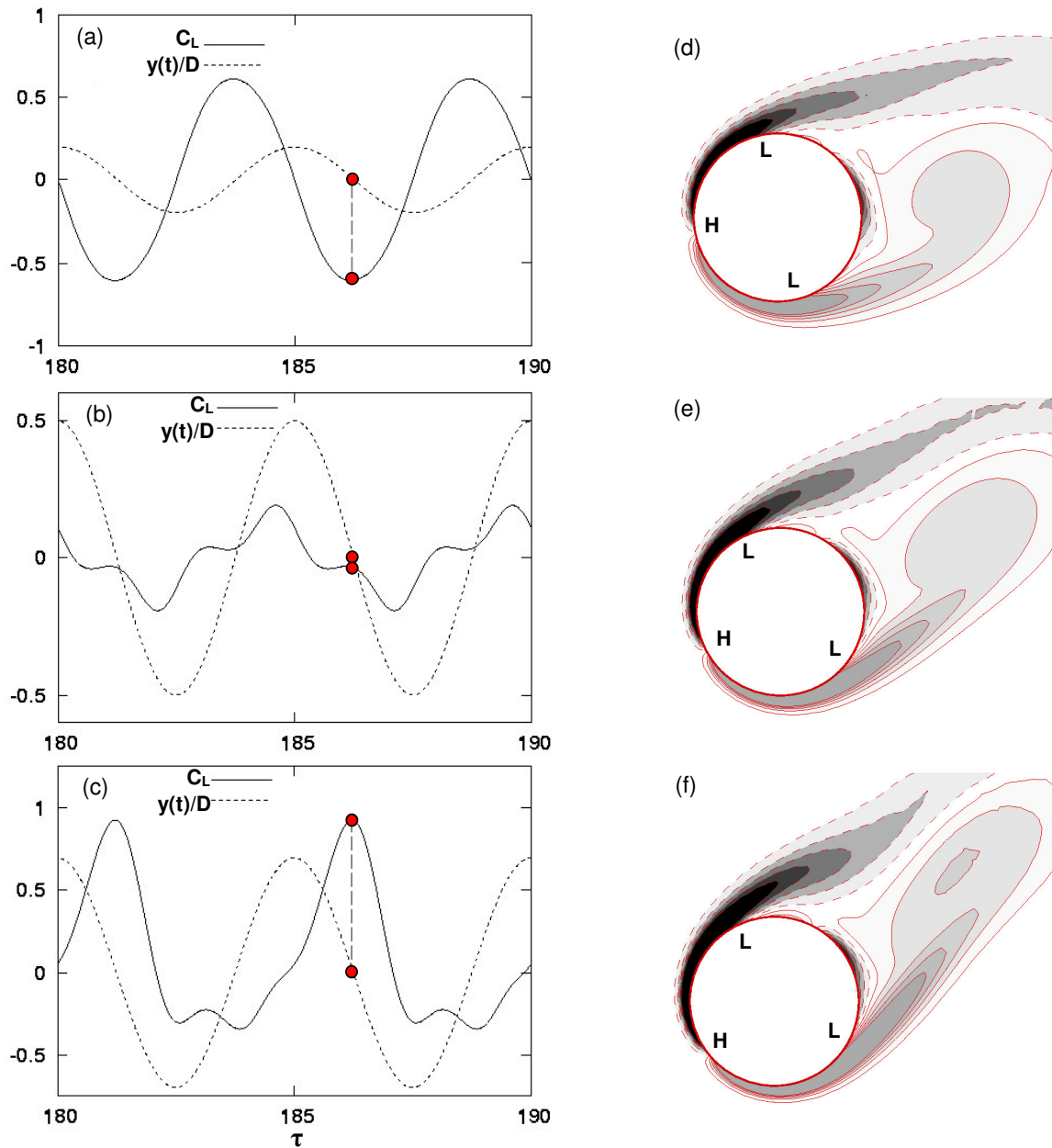


Figure 2. Lift coefficients and corresponding vorticity contours for cylinder oscillating at $V_i=5.0$, (a) $A/D=0.199$, (b) $A/D=0.497$ and (c) $A/D=0.696$. Red dots indicate point at which images were obtained. Negative vorticity is shown in black and enclosed by dashed contours. H and L show high and low pressure regions respectively.

force (C_L negative). This differed from the wake structure at amplitudes near 0.5 (figure 2(e)), when the front stagnation point was shifted towards the bottom of the cylinder. This high pressure region partially offset the low pressure created in the lower shear layer, resulting in a near zero value for C_L .

At amplitudes in the region of 0.7 the P+S mode of shedding occurred and the elongated region of positive vorticity shown in figure 2(f) separated into two distinct vortices downstream. The elongation of the lower shear structure moved the concentration of vorticity further from the cylinder and the low pressure in the upper shear layer dominated, giving a maximum positive C_L . During the upwards motion of the cylinder in this asymmetric wake mode, negative vorticity from the upper shear layer formed a low pressure region much closer to the back of the cylinder. This contributed a larger component to the upward lift, resulting in the net downward lift being of much lower amplitude than the net upward lift generated in the previous half cycle.

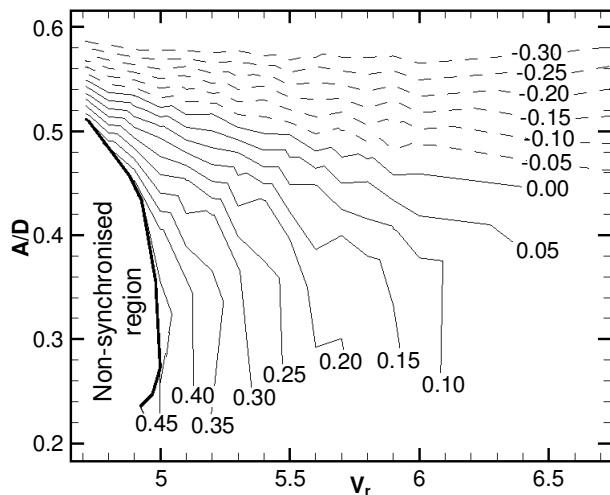


Figure 3. Contours of constant energy transfer in the primary lock-in region. Values of E are shown and negative energy transfer is indicated with dashed lines

From energy measurements throughout the lock-in region contours of energy transfer per cycle were established (figure 3). These contours of energy, E , indicated that the energy transition took place between amplitudes of 0.45 and 0.55. For VIV to occur a positive energy transfer is required to account for losses due to structural damping [3,6], hence this boundary represents an upper limit to the observed oscillation amplitude. At amplitudes above the energy transition, values of E became steadily more negative and were dependent primarily on the amplitude, rather than the reduced velocity. This may be linked to findings in [9] where the P+S wake developed at an almost constant amplitude. The current investigation did not examine the wake mode transition in any detail but it is intended that future work will define this boundary more clearly. The flattened nature of the zero-energy contour may also be representative of the fact that the upper branch of response (see [11] for details) was undetected in the two-dimensional investigation. This was not the case in [6] where a sharp peak occurred in the energy contours for V_r between 5.0 and 6.0.

Conclusions

Following an investigation of two-dimensional flow past an oscillating cylinder at $Re=200$, information was obtained for the lift force and wake mode occurring at various frequencies and amplitudes of motion. The region in which vortex shedding locked-on to the cylinder motion was determined and energy transfer calculated for all points in the synchronized region. Following analysis of the wake modes, it was discovered that the Kármán shedding displayed a gradual decrease in energy transfer as the reduced velocity and amplitude increased. This was brought about by the development of two secondary peaks in the lift force. At a critical amplitude, these peaks switched prominence, effecting a shift in phase between lift and displacement, and a change in direction of energy transfer. Further increase in amplitude saw the onset of asymmetric P+S shedding in regions of negative energy transfer and amplitudes above 0.6. A plot of energy contours (figure 3) indicated that an energy transition took place over a fairly small range of amplitudes in the primary lock-on region. This result indicated the occurrence of maximum VIV amplitudes of between 0.45 and 0.55 at reduced velocities between 4.5 and 6.5.

References

- [1] Bishop, R.E.D. and Hassan, A.Y., The Lift and Drag Forces on a Circular Cylinder Oscillating in a Flowing Fluid, *Proc. R. Soc. Lond. A*, **277**, 1964, 51-75.
- [2] Blackburn, H.M. and Henderson, R.D., A Study of Two-Dimensional Flow Past an Oscillating Cylinder, *J. Fluid Mech.*, **385**, 1999, 255-286.
- [3] Carberry, J., Sheridan, J. and Rockwell, D., Forces and Wake Modes of an Oscillating Cylinder, *J. Fluids Struct.*, **15**, 2001, 523-532.
- [4] Griffin, O.M., The Unsteady Wake of an Oscillating Cylinder at Low Reynolds Number, *J. Appl. Mech.*, **38**, 1971, 729-738.
- [5] Griffin, O.M. and Ramberg, S.E., The Vortex-Street Wakes of Vibrating Cylinders, *J. Fluid Mech.*, **66**, 1974, 553-576.
- [6] Hover, F.S., Techet, A.H. and Triantafyllou, M.S., Forces on Uniform and Tapered Cylinders in Crossflow, *J. Fluid Mech.*, **363**, 1998, 97-114.
- [7] Koopmann, G.H., The Vortex Wakes of Vibrating Cylinders at Low Reynolds Numbers, *J. Fluid Mech.*, **28**, 1967, 501-512.
- [8] Lu, X.-Y. and Dalton, C., Calculation of the Timing of Vortex Formation From an Oscillating Cylinder, *J. Fluids Struct.*, **10**, 1996, 527-541.
- [9] Meneghini, J.R. and Bearman, P.W., Numerical Simulation of High Amplitude Oscillatory Flow About a Circular Cylinder, *J. Fluids Struct.*, **9**, 1995, 435-455.
- [10] Thompson, M.C., Hourigan, K. and Sheridan, J., Three-Dimensional Instabilities in the Wake of a Circular Cylinder, *Exp. Therm. Fluid Sci.*, **12**, 1996, 190-196.
- [11] Williamson, C.H.K. and Govardhan, R., Vortex-Induced Vibrations, *Ann. Rev. Fluid Mech.*, **36**, 2004, 413-455.
- [12] Williamson, C.H.K. and Roshko, A., Vortex Formation in the Wake of an Oscillating Cylinder, *J. Fluids Struct.*, **2**, 1988, 355-381.